

# A SPATIAL STRUCTURE OF A FLOW OF AXISYMMETRIC SUDDEN EXPANSION

**Noriyuki Furuichi and Yasushi Takeda**

Paul Scherrer Institut  
CH5232 Villigen PSI, Switzerland  
Noriyuki.Furuichi@psi.ch, Yasushi.Takeda@psi.ch

**Masaya Kumada**

Gifu Univ.  
1-1 Yanagido, Gifu, 501-1193, Japan  
kumada@cc.gifu-u.ac.jp

## ABSTRACT

A flow transition for an axisymmetric sudden expansion was experimentally investigated. Spatio-temporal flow field measured using ultrasonic velocity profiler and analyzed by a two-dimensional Fourier transform and a proper orthogonal decomposition. The variation of the zero-cross point of the axial velocity distribution, the energy of velocity fluctuation directed to upstream and the eigenmode spectrum have the same transitional scheme with respect to Reynolds number. The transitional scheme can be classified as laminar flow for  $Re_d < 1000$ , and transitional regime for  $Re_d = 1000-4000$  and turbulent regime for  $Re_d > 4000$ . We found that the two large change occurs in the transitional regime at around  $Re_d = 1500$  and  $2000$ . The jump that occurs at  $Re_d = 2000$  is caused by the change of the flow condition in the upstream pipe. The jump at  $Re_d = 1500$  shows a change of the spatial structure of the flow.

## INTRODUCTION

A flow structure in a pipe with a symmetric sudden expansion has been studied in the past as it is frequently encountered in engineering practice. Concerning the fundamental fluid mechanical characteristics in this configuration, it has a complexity of the internal flow separation and reattachment.

It is well known that a time averaged reattachment length varies as a function of a Reynolds number. Some researchers investigated its behavior because it is one of the most important features of this flow field (Back and Roschke 1972, Eaton and Johnston 1981, Armly et al. 1983, Adams and Johnston 1988). The averaged reattachment length increases steadily for laminar regime ( $Re \leq 10^3$ ) and decreases in the transitional regime. At higher Reynolds number ( $Re \geq 10^4$ ; turbulent regime), it increases slightly with increasing Reynolds number. The flow mechanism of the laminar and turbulent regime have already been understood quantitatively well. For a laminar region,

the averaged reattachment length obtained by recent numerical experiments is in a good agreement with those by experiments. (Lewis and Pletcher 1986, Abe et al 1994). On the other hand, for a transitional regime, the averaged reattachment length have large difference among many experiments. A behavior of variation of the reattachment length as a function of Reynolds number of this regime shows complex change as reported by Armly et al.(1983), but it has not been investigated enough by taking into account a change of the spatial structure.

It is also well known that there exists a low-frequency stationary motion, usually called "flapping" of the separated shear layer. This phenomenon appears to be strongly related to a concentration of the separated shear vortex and the fluctuation of the instantaneous reattachment point (Driver et al, 1985). In many previous reports, the experimental results such as velocity profile or turbulent intensity were obtained as a function of wall normal direction (like  $v_z(r)$ ). Moreover, no temporal characteristics were considered. However, for investigating detail structure of the flapping in relationship with the reattachment, it is necessary to obtain a streamwise velocity distribution as a function of streamwise direction and time (like  $v_z(z,t)$ ).

In this investigation, we used a ultrasonic velocity profiler (UVP) to obtain spatio-temporal velocity fields on the streamwise direction ( $v_z(z,t)$ ) in the axisymmetric sudden expansion and analyzed them by a two-dimensional Fourier transform and the proper orthogonal decomposition (POD method). Since various modes can be observed in this flow field such as flapping, growth and shedding of the separated shear vortex and recirculation flow, it is important to analyze the flow field by making use of field decomposition by these methods. We investigated a behavior of transition sequence of the flow field from laminar to turbulent regime by evaluating the contribution of each modes to the total turbulent energy.

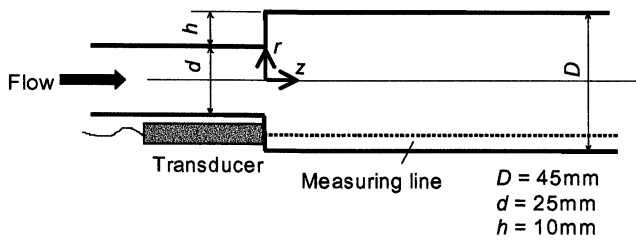


Figure 1. Experimental setup

## EXPERIMENTAL SETUP AND METHOD

Experimental apparatus and coordinate system is illustrated in Figure 1. The pipe diameter of the upstream of the step is  $d=25\text{mm}$  and is  $D=45\text{mm}$  at downstream. The step height is then  $h=10\text{mm}$  and the expansion ratio is  $ER=1.8$ . The sudden expansion is located at  $84d$  downstream from the flow conditioner. The control parameter is  $Re_d = dV_b/v = 5.0 \times 10^2 \sim 1.5 \times 10^4$ , where  $d$  is the upstream pipe diameter and  $V_b$  a bulk velocity estimated from flow rate. The velocity profile in the upstream channel before entering the sudden expansion is fully developed and the critical Reynolds number is  $Re_c \approx 2.0 \times 10^3$  in this experiment.

The measurements were carried out with an ultrasound velocity profiler (Takeda, 1990) which can obtain time series of instantaneous velocity profiles. One instantaneous velocity profile consists of 128 data points. The ultrasonic transducer was set at  $r/h=1.75$  as shown in the Figure 1 and measured a streamwise velocity component ( $v_z$ ) as a function of  $z$  and time ( $v_z(z,t)$ ). The distance between two measurement points is  $1.48\text{mm}$  and measured range is  $z/h=2\sim 20$ . A typical time to obtain one velocity profile is about  $70\text{msec}$  and total measuring time is  $573\text{ second}$  ( $8192$  profiles).

## RESULT AND DISCUSSION

### Velocity field – Average profile

Before discussing spatio-temporal nature of the flow, we start to use time averaged velocity profiles. A typical example is given in Figure 2 together with turbulent intensity at  $Re_d=3591$ . It shows a smooth velocity profile. In most of previous works, the averaged velocity profile was measured as a function of wall-normal axis as  $V_z(r)$ , and then the measurement points for streamwise direction was very coarse. A typical velocity profile has two regions of positive and negative velocity values. It is easily justified that the region of negative velocity corresponds to a so-called recirculation bubble, and its spatial structure can be evaluated quantitatively from a zero-cross point of those averaged profiles.

A behavior of a reattachment phenomenon is normally characterized by a reattachment length. Many of the previous investigations performed measurements of a variation of the reattachment length as a function of a Reynolds number. However an increment of the measured Reynolds number is

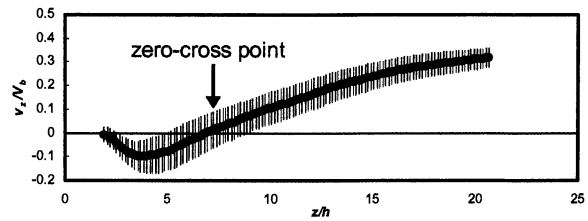


Figure 2. Example of an averaged velocity profiles at  $Re_d=3591$

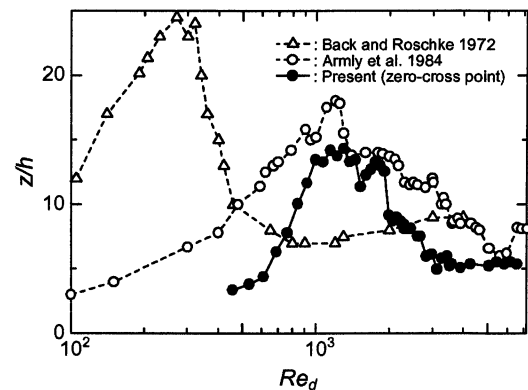


Figure 3. Variations of the zero-cross point and the reattachment point

large. The most detailed work might be of Armly et al(1984) on two-dimensional backward-facing step. They measured a reattachment length for a wide range of Reynolds number using laser Doppler anemometry. They summarized the tendency of the variation of the reattachment length as following (cf. Figure 3); The laminar regime of the flow is characterized by a reattachment length that increases with Reynolds number (based on the hydraulic diameter). The regime of transitional flow ( $Re=1200\text{-}6000$ ) is characterized by a sharp decrease in the reattachment length, by irregular decrease to a minimum value at a Reynolds number of approximately  $5500$ , then an increase to a constant level. The turbulent regime is then characterized by a constant reattachment length.

We measured streamwise velocity profiles with much finer distance of data points of  $z$  so that we can obtain the zero-cross point of the velocity profile, as shown in Figure 2, with much higher precision. Although this value is not the same physical value as a reattachment length because its radial position of the ultrasonic beam is slightly away from the wall, it can be compared reasonably with other investigations. Figure 3 shows a variation of the zero-cross point. The general tendency of the variation of the zero-cross point is in good agreement with a change of reattachment length (Armly et al.). For a region from  $Re_d=1000\text{-}2000$ , there are two maxima. The first maximum is seen at  $Re_d \approx 1500$ , and the second at  $Re_d \approx 2000$ . The second might be due to the change of upstream flow condition to turbulence since it happens at a critical Reynolds number of

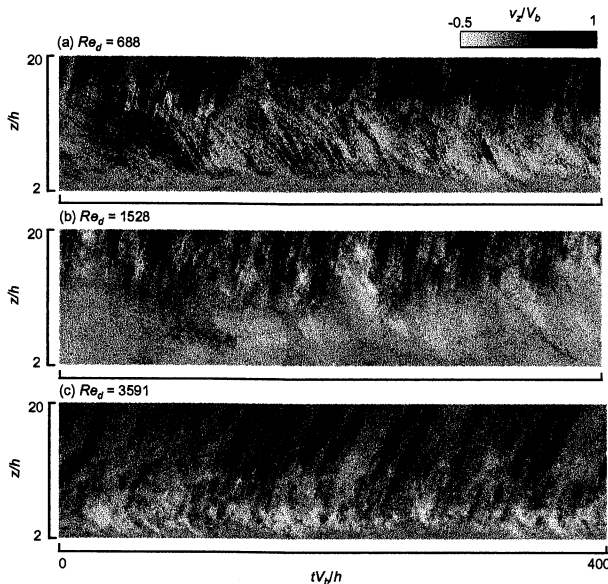


Figure 4. Examples of measured velocity fields

about 2000. However, the mechanism of the first increase can not be explained from the averaged velocity profile. For  $Re_d = 2000-4000$ , it decreases irregularly and is considerably stable for  $Re_d > 4000$ . For a later discussion, we call the regime of  $Re_d < 1000$  a laminar regime,  $Re_d = 1000-3000$  a transitional regime,  $Re_d > 3000$  a turbulence regime.

### Spatio-temporal velocity profile

As examples of the spatio-temporal velocity field, a two-dimensional gradation map of  $v_z(z, t)$  velocity a component are shown in Figure 4. The horizontal axis is a normalized time and vertical axis is a position normalized by a step height. The gradation changes from white to black as increasing velocity. The stripes of positive gradient means a flow (vortices) directed to downstream and one of negative gradient means a upstream flow. With an overall view, vortices are traveling to downstream for  $z/h = 10 \sim 20$ . A large scale structure around the separated shear layer is observed for  $z/h = 5 \sim 10$ , where the flow direction changes as time, namely a strong spatial fluctuation of instantaneous zero crossing point. These figures show clearly a change of such a flow structure in each regime. The recirculation region observed in the Figure (b) is larger than that in (a) as increasing Reynolds number. It becomes smaller and the gradient of the stripes is smaller in figure (c).

Examples of the local power spectra of the streamwise velocity fluctuation are shown in Figure 5. The Reynolds number and the spatial location are given in the figure. These locations correspond to the averaged zero-cross point. Although it is said that the low-frequency fluctuation is dominant in these locations (around a reattachment region), we found that no typical peak can be seen for these Reynolds number.

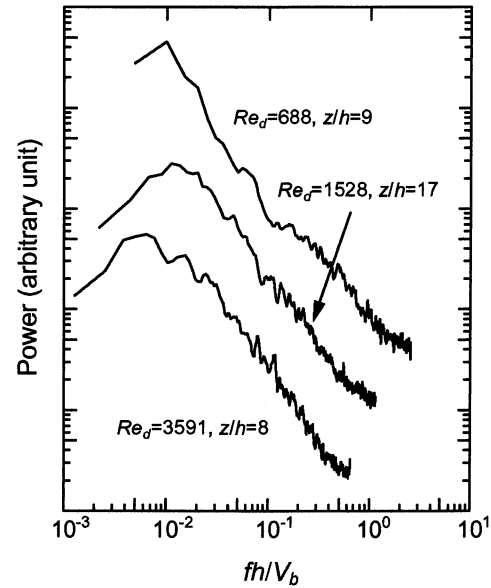


Figure 5. Example of the power spectra of the velocity fluctuation

### Two-dimensional Fourier transform

As shown in Figure 4, a structure of which motion directs to downstream and upstream exists in the same region of the flow field. The vortex shed from the separated shear layer travels to downstream, while a part of recirculation bubble flows to upstream, and as a result its boundary and the reattachment point fluctuates in spatio-temporal manner. For investigating quantitatively the nature of this complicated flow field, a time-domain Fourier analysis (power spectra) is not sufficient as shown in Figure 5. We then used a two-dimensional Fourier analysis. As the energy of velocity fluctuation traveling to downstream and upstream can be obtained separately by this method, it would be suited for analysis of this flow field. We computed the spectrum of the velocity fluctuation by following formula.

$$S(k, f) = \int_{-\infty}^{\infty} \int_{-\infty}^{\infty} v_z(z, t) e^{-ikz} e^{-ift} dz dt \quad (1)$$

where  $f$  is frequency and  $k$  is wave number. With respect to the space and time resolution, we can obtain a two-dimensional Fourier spectrum on the plane of  $f = [0, 7.042](\text{Hz})$  and  $k = [0, 0.337](\text{mm}^{-1})$  with resolution of  $[0.013\text{Hz}, 0.003\text{mm}^{-1}]$ .

Examples of the spectra of the two-dimensional Fourier transform are shown in Figure 6. The abscissa is frequency and the coordinate is wave number. Negative value of the wave number is also plotted so that flow direction can be accounted. Namely, the first domain depicts the spectrum of the flow that directs to downstream and the forth is to upstream. Reflecting the velocity fluctuation caused by the vortex that is traveling to downstream with

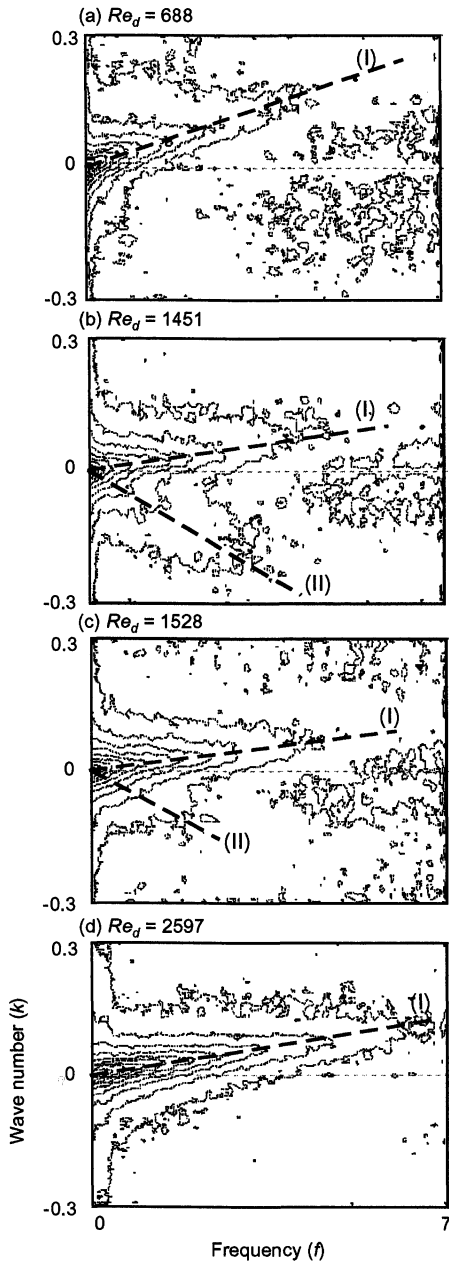


Figure 6. Contour maps of the two-dimensional Fourier transform

constant velocity, the energy concentration is shown clearly on each figures as a line (shown as (I)). In (b), by comparing figure (a), a line of negative gradient appears (dotted line; II), which corresponds to the flow directed to upstream. This feature can also be seen in figure (c), which is much smaller than in (b). In the turbulent regime (figure (d)), the energy is more concentrated on the vortex structure and no upstream flow is observed. It is, concludingly, clear that it is a characteristic phenomenon appearing only in the transition regime.

A gradient of the lines on the two-dimensional Fourier spectrum corresponds to the convection velocity of the vortex traveling to downstream. The variation of the convection velocity thus estimated from those spectra is shown in Figure 7. In the laminar and the transitional regime, the obtained

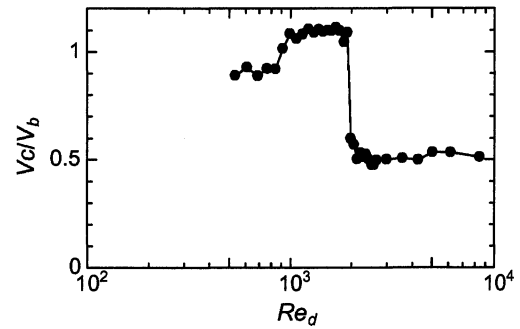


Figure 7. Convection velocity directed to downstream (normalized by the bulk velocity)

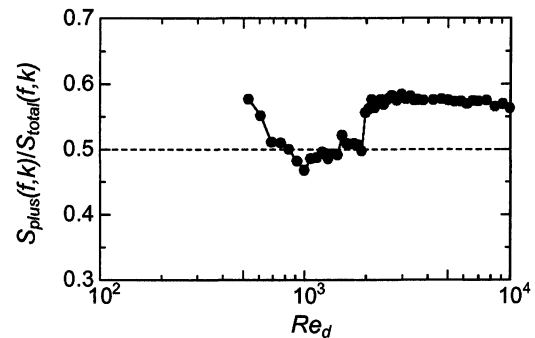


Figure 8. Relative power of velocity fluctuation directed to downstream

convection velocity is more or less equal to the main flow. This indicates that the vortex shedding is caused by the shear layer. On the other hand, it shows a sudden change at  $Re_d \approx 2000$  down to the half of the bulk velocity, indicating a generation of larger vortex outside the shear layer. This result for the turbulent regime is in good agreement with the previous reports. (Hijikata et al. 1990, Furuichi et al. 1999).

To observe a contribution of the energy for each direction, a variation of the energy of flow directed to downstream relative to the total energy is shown in Figure 8. The total energy is defined as the summation of  $S(f,k)$  over the whole domain and the energy directed to downstream is a summation of the power in the first domain. The transition behaviour is seen also in this figure; similar to the variation of the zero-cross point. The fraction of the energy directed to downstream decreases at  $Re_d \approx 1000$ , and is almost constant for  $Re_d = 1000-2000$  except for a small jump at  $Re_d = 1500$ . There is observed a large jump at  $Re_d = 2000$ . It corresponds to the sharp decrease of the zero-cross point shown in Figure 3.

Figure 9 shows reconstructed spatio-temporal velocity fields. These velocity fields are reconstructed only for the flow directed to downstream of which the convection velocity is (a)  $1.1V_b$  and (b)  $0.5V_b$  (all other component is filtered out). It shows clearly a vortex motion that is traveling to downstream and the difference of the convection velocity between two flow regimes. In figure (a), this motion has a fairly high periodicity and estimated Strouhal number  $St = fh/V_b = 0.2$ , where  $f$  was estimated from power

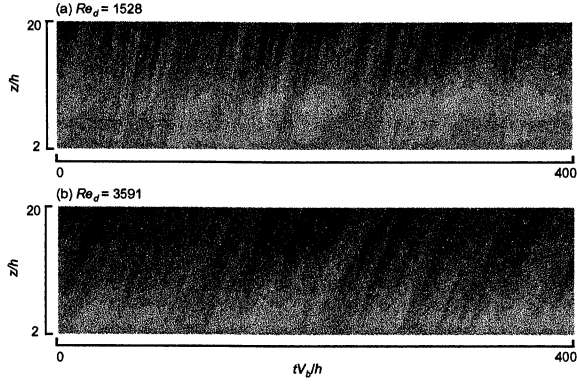


Figure 9. Reconstructed velocity field

spectrum of this velocity profile. On the other hand, periodical structure is weak in figure (b) and the low frequency fluctuation is dominant ( $St=0.02$ ). This is consistent with previous investigations by Eaton & Johnston (1981).

### Orthogonal decomposition

As discussed earlier, this flow field is less periodic in spatial and/or temporal domain so that Fourier analysis is less effective. To identify the coherent structure of this flow field, the POD (proper orthogonal decomposition) method would be better suited since the dominant structure involves higher engenmodes. At the same time, the eigenspectrum might be used to investigate the change of the structure. The method is based on the decomposition of the fluctuating velocity field into a sum of mutually orthogonal engenfunctions of the two-point correlation tensor. This method has been applied by many researchers to various flow fields. (Delville et al. 1990, Takeda 1999)

We decomposed the streamwise velocity field ( $z$ - $t$  field) by the following formula;

$$v(z,t) = \sum_n a^{(n)}(t)\phi^{(n)}(z) \quad (2)$$

where  $\phi^{(n)}(z)$  are eigenfunctions,  $a^{(n)}(t)$  are uncorrelated random coefficients of eigenvalues ( $\lambda^{(n)}$ ). The contribution of each structure to the turbulent kinetic energy and total energy ( $E$ ) in the measurement region ( $D:z/h=2-20$ ) can be determined as

$$\langle v^2(z) \rangle = \sum_n \lambda^{(n)} \phi^{(n)2}(z) \quad (3)$$

$$E = \int_D v^2(z) dz = \sum_n \lambda^{(n)} \quad (4)$$

The variation of eigenvalues for the first 10 strongest modes is shown in Figure 10 with respect to Reynolds number. The 0th mode decreases in laminar regime and other modes increase as increasing Reynolds number. In the transitional regime, the eigenvalue of 0th and 1st modes jump up at  $Re_d=2000$ . This corresponds to a large change in

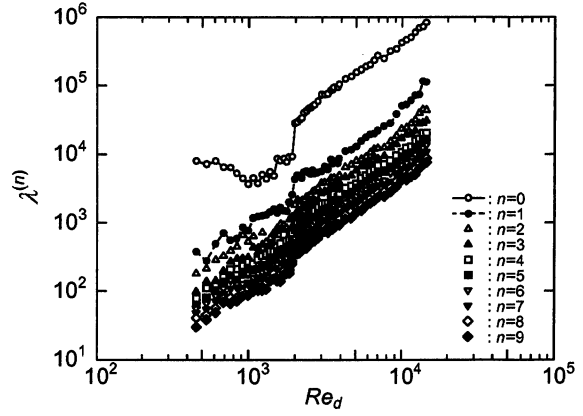


Figure 10. Variation of 10 eigenvalues

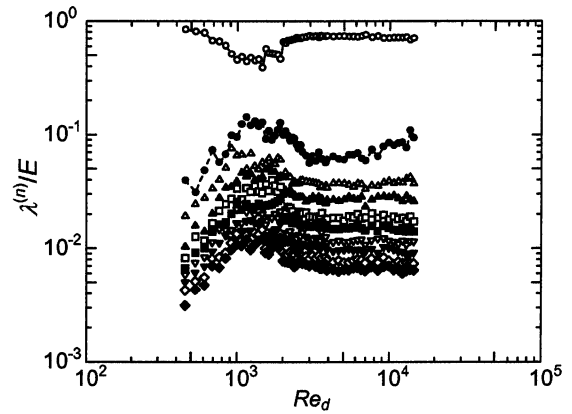


Figure 11. Variations of normalized eigenvalue

the reattachment length at this Re number; see Figure 3. Furthermore, there is seen a smaller jump at  $Re_d=1500$ . This feature of two step increase of eigenvalues appears to correspond to the existence of two maxima in the variation of the reattachment length. For the turbulent regime ( $Re_d>3000$ ), the energy increases steadily and no large change is seen.

In order to see a contribution of the energy of each mode, the variation of the eigenvalues for the first 10 eigenmodes normalized by the total energy of the eigenvalues ( $\lambda^{(n)}/E$ ) is plotted in Figure 11. For laminar regime, the fraction of the energy of the 0th mode decreases while those of other modes increase with Reynolds number. In the transition regime, it is clearly seen that the energy of 0th mode decreases while those of higher modes increases, showing a local minimum for 0th mode and local maxima for other modes. This indicates that a considerably large fraction of total energy is occupied by higher modes. It may imply an energy transfer from the base mode to the higher mode in this regime.

Aubry et al.(1994) proposed another way to use the information in the eigenvalue spectrum to identify changes in flow behavior as following formula

$$H = -\frac{1}{\ln N} \sum_n p^{(n)} \ln p^{(n)} \quad (5)$$

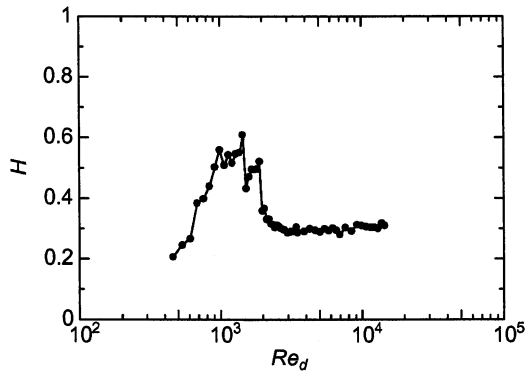


Figure 12. A variation of the global entropy

where  $H$  is a global entropy and  $p^{(n)} = \lambda^{(n)}/E$ .  $N$  is the number of data points.  $H=0$  corresponds to perfectly ordered state and  $H=1$  corresponds to the completely disordered state. A variation of the global entropy of our data is shown in Figure 12 with respect to Reynolds number. It shows also a typical transitional scheme as discussed above. Namely  $H$  is large for the transition regime with two maxima. For the laminar regime, the global entropy increases steadily, and for  $Re_d > 3000$ , it is quite constant.

## CONCLUSION

Spatio-temporal velocity field of the axiymetric sudden expansion was experimentally investigated using ultrasonic velocity profiler and analyzed by two-dimensional Fourier transform and proper orthogonal decomposition to investigate transitional scheme of the spatial structure.

The zero-cross point for  $Re_d < 1000$  increases steadily as increasing Reynolds number. It decreases suddenly at two Reynolds numbers, at  $Re_d = 1500$  and  $2000$ . For  $Re_d = 2000-3000$  it decreases slightly and  $Re_d > 3000$  it stays constant.

A variation of the energy of the velocity fluctuation directed upstream and downstream was studied using two-dimensional Fourier transform. It has also the same transitional scheme as that of the zero-cross point. POD was also performed. It was found that there are two local maxima at  $Re_d = 1500$  and  $2000$  in the variation of fractional energy with Reynolds number. This is also observed in the variation of global entropy. The first jump at  $Re_d = 1500$  indicates clearly a change of the spatio-temporal structure in the transitional scheme. The second jump at  $Re_d = 2000$  might be caused by the change of the flow condition upstream pipe.

## References

Abe, K., Kondoh, T., Nagano, Y., A new turbulence model for predicting fluid flow and heat transfer in separating and reattaching flows - I. Flow field calculations, *Int. J. Heat Mass Transfer*, 37, 139-151, 1994

Adams, E.W., Johnston, J.P., Effects of the separating shear layer on the reattachment flow

structure, Part2:Reattachment length and wall shear stress, *Exp. In Fluids*, 6, 493-499, 1988

Armly, B.F., Durst, F., Pereira, J.C.F., Schönung, B., Experimental and theoretical investigation of backward-facing step flow, *J. Fluid Mech.*, 127, 473-496, 1983

Aubry, N., Chauve, M.P., Guyonnet, R., Transition to turbulence on rotating flat disk, *Phys. Fluids*, 6, 2804-2814, 1994

Back, L.H., Roschke, E.J., Shear-layer flow regimes and wave instabilities and reattachment lengths downstream of an abrupt circular channel expansion, *J. of Applied Mech.*, 39, 677-681, 1972

Delville, J., Bellin, S., Bonnet, J.P., Use of the proper orthogonal decomposition in a plane turbulent mixing layer, *Turbulence and Coherent Structures*, 75-90, 1990

Driver, D.M., Seegmiller, H.L., Marvin, J.G., Time-dependent behavior of a reattachment shear layer, *AIAA J.*, 25, 7, 914-919, 1987

Eaton, J.K., Johnston, J.P., A review of research on subsonic turbulent flow reattachment, *AIAA J.*, 19, 1093-1100, 1981

Furuichi, N., Hachiga, T., Hishida, K., Kumada, M., A vortex structure of a two-dimensional backward-facing step by using advanced multi-point LDV, Proc. of 1 st symposium of Turbulence and Shear Flow Phenomena, 1045-1050, 1999

Hijikata K., Mimatsu, J., Inoue, J., A study of wall pressure structure in a backward step flow by a holographic / velocity-pressure cross-correlation visualization, *ASME-FED*, 128, Experimental and Numerical Flow Visualization, 61-68, 1991

Lewis, J.P., and Pletcher, R.H., Limitations of the boundary-layer equations for predicting laminar symmetric sudden expansion, *J. of Fluid Eng.*, 108, 208-213, 1986

Takeda, Y., Development of ultrasound velocity profile monitor, *Nuc. Eng. Des.*, 126, 177-284, 1990

Takeda, Y., Quasi-periodic state and transition to turbulence in a rotating Couette system, *J. Fluid Mech.*, 389, 81-99, 1999